SCIENTIFIC REPORTS

OPEN

SUBJECT AREAS:
ELECTRONIC DEVICES
APPLIED PHYSICS

Received
16 October 2013

Accepted
9 December 2013

Published
8 January 2014

Wafer-Scale Integration of Graphene-based Electronic, Optoelectronic and Electroacoustic Devices

He Tian[1,2], Yi Yang[1,2], Dan Xie[1,2], Ya-Long Cui[1,2], Wen-Tian Mi[1,2], Yuegang Zhang[3,4] & Tian-Ling Ren[1,2]

[1]Institute of Microelectronics, Tsinghua University, Beijing 100084, China, [2]Tsinghua National Laboratory for Information Science and Technology (TNList), Tsinghua University, Beijing 100084, China, [3]The Molecular Foundry, Lawrence Berkeley National Laboratory, 1 Cyclotron Road, Berkeley, CA 94720, USA, [4]Suzhou Institute of Nano-Tech and Nano-Bionics, Chinese Academy of Sciences, Suzhou 215123, China.

Correspondence and requests for materials should be addressed to Y.Z. (yzhang5@lbl.gov) or T.-L.R. (RenTL@tsinghua.edu.cn)

In virtue of its superior properties, the graphene-based device has enormous potential to be a supplement or an alternative to the conventional silicon-based device in varies applications. However, the functionality of the graphene devices is still limited due to the restriction of the high cost, the low efficiency and the low quality of the graphene growth and patterning techniques. We proposed a simple one-step laser scribing fabrication method to integrate wafer-scale high-performance graphene-based in-plane transistors, photodetectors, and loudspeakers. The in-plane graphene transistors have a large on/off ratio up to 5.34. And the graphene photodetector arrays were achieved with photo responsivity as high as 0.32 A/W. The graphene loudspeakers realize wide-band sound generation from 1 to 50 kHz. These results demonstrated that the laser scribed graphene could be used for wafer-scale integration of a variety of graphene-based electronic, optoelectronic and electroacoustic devices.

Graphene, a kind of two dimensional material, has attracted great interest of researchers due to its outstanding properties[1], such as ultrahigh mobility[2], mechnical strength[3], thermal conductivity[4] and transprancy[5]. However, its zero badgap makes it not suitable for low power electronic applications[6]. Graphene oxide (GO) is another attractive materials since it has a badgap larger than 0.5 eV[7]. The most attractive property of GO is that it can be (partly) reduced to graphene. The reduced GO (rGO) is usually considered as semiconductor or semimetal[8]. The eletrical conductivity is tunable by changing the oxygen contents in rGO. Zhongqing Wei et al. reported a nanoscale local thermal reduction of GO with a heated atomic force microscopetip[9]. Recently, Wei Gao et al. reported a direct laser reduction of GO to realize micro-supercapacitors on hydrated graphite oxide films[10]. Lately, Richard B. Kaner et al.[11] utilized the DVD laser scribing technology to realize micro-supercapacitors with a power density of $\sim$200 Wcm^{-3}, which is among the highest values achieved for any supercapacitor. However, the functionality of the graphene devices is still limited[12] owing to the restriction of the high cost, the low efficiency and the low quality of the graphene growth and patterning techniques.

In this work, the integrated wafer-scale in-plane transistors, the photodetectors and the loudspeakers by laser scribing technology are proposed. This is a substantial novel research study that has several approaches. Firstly, the in-plane graphene transistor has a large on/off ratio up to 5.34. This parameter is much higher than that of most CVD graphene (I_{on}/I_{off} ratio $\sim$1.04 $\sim$ 1.4)[13–15]. Secondly, the graphene photodetectors with photo responsivity and specific detectivity as high as 0.32 A/W and 4.996×10^{10} $cmHz^{1/2}W^{-1}$ under 0.1 V bias were achieved. As far as we know, this is the first demonstration of 1-dimentional and 2-dimentional array of graphene photodetectors for photo imaging. Thirdly, the laser scribed graphene is also demonstrated to be a high performance loudspeaker with wide-band sound generation from 1 to 50 kHz. The sound generation spectrum (1–50 kHz) is 2.5 times wider than that of reported mono-layer graphene on PDMS (1–20 kHz)[16].

Laser scribing is an attractive pattering technology due to its low-cost and time-efficient fabrication process. The one-step laser scribing technology allows transfer-free graphene synthesis directly on flexible substrates or uneven substrates. In general, CVD-synthesized graphene devices usually require tens of hours for graphene growth, transfer, and patterning, and the flat target transfer substrate is preferred. By using this new laser scribing

technology, wafer-scale graphene patterns can be obtained in ~25 minutes. Without coating photoresist for lithography, the surface of patterned graphene remains as clean as its pristine status. The results suggest that the laser scribing technology can potentially produce more economical and time-saving graphene-based circuits/systems for practical applications. It is believed that the proposed laser scribing technology could also have broad prospective applications in the graphene-based electronics, sensors and actuators systems.

Results

Scalable fabrication of laser scribed graphene. The scalable fabrication of laser scribed graphene is depicted in Figure 1. The DVD burner containing light scribe function has been used. The 788 nm laser pulses with 5 mW maximum power produced by the burner could convert the stack single-layer GO film into graphene (Figure 1a). A designed patterning with grayscale, which could control the DVD drive for selective reduction of GO, was import to the software in order to control the patterning position and laser intensity. As shown in figure 1b, wafer-scale in-plane transistor patterns are designed. After importing the electronic file into the computer software and ~25-minute laser scribing in DVD burner, graphene transistors are directly patterned on a GO film (Figure 1c). Figure 1d shows the logo of Tsinghua University and the corresponding graphene pattern on the GO film (Figure 1e). A colored picture and the corresponding laser scribed graphene patterning gray scale are given in Figures 1f and 1g. Figure 1h and 1i show an array of graphene transistors, an array of photodetectors, and a graphene loudspeaker device integrated on a flexible substrate by the direct laser scribing method. The wafer-scale fabrication flexible graphene-based devices after peeling off with the PET substrate from the DVD disc is shown in Figure 1j.

Morphology and structure of laser scribed graphene. To investigate the morphology and structure change of the GO film before and after laser scribing, the characterization were performed with SEM, Raman and XPS. The morphology and structure of the laser scribed graphene and the GO film is illustrated in Figure 2. Figure 2a is the SEM image of laser scribed graphene surface under low magnification. The laser scanning direction is also shown and the patterning resolution is ~20 μm. Porous structure could be identified in the SEM image of laser scribed graphene surface under high magnification (Figure 2b). And this could be mainly attributed to the Joule heating that induces the local film

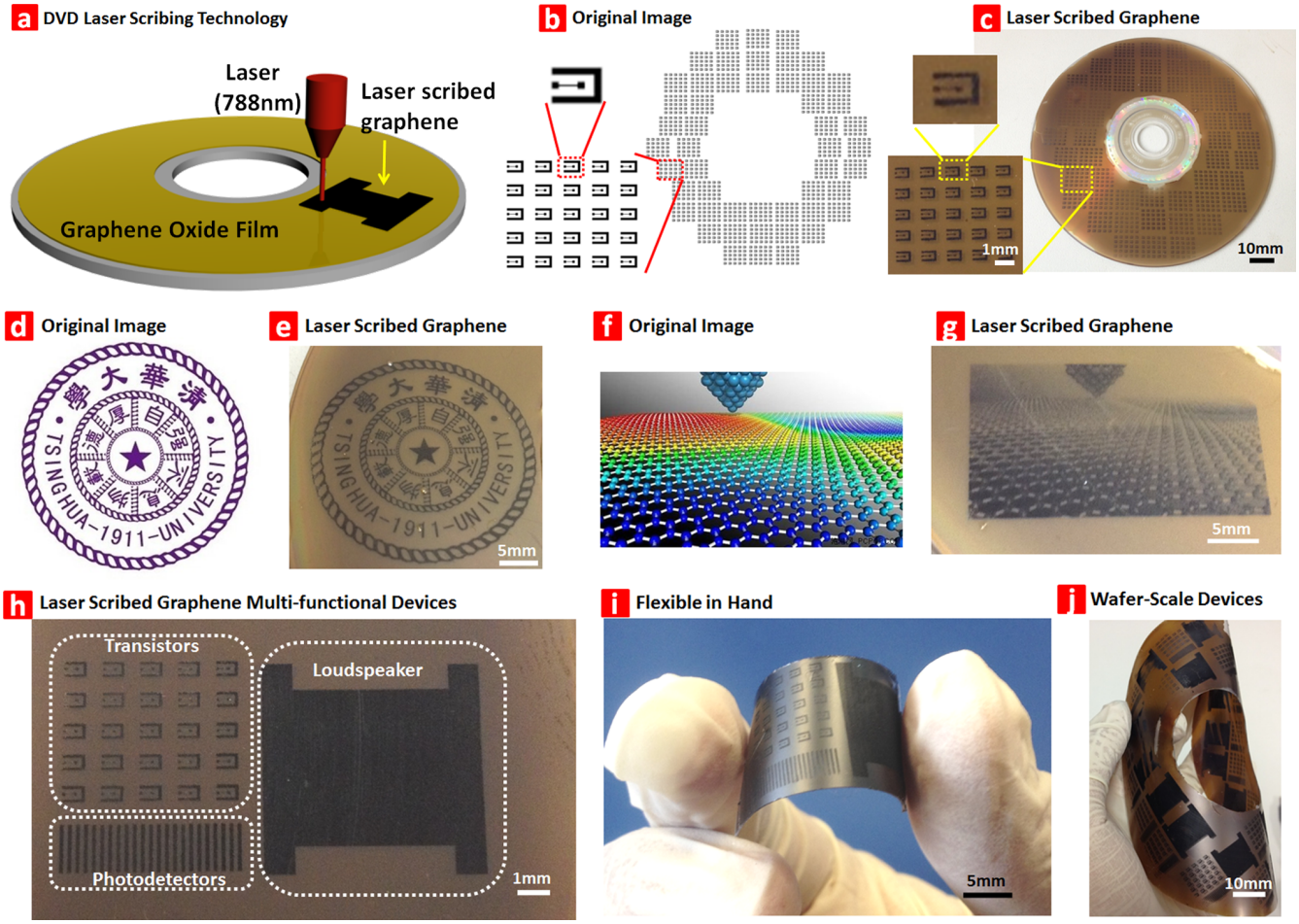

Figure 1 | Scalable fabrication of laser scribed graphene. (a) A schematic diagram showing the fabrication process of laser scribed graphene. A GO film is coated on a DVD media disc. The disc is inserted into a LightScribe DVD drive and a computer-designed circuit is etched onto the film. The laser inside the drive converts the golden-brown GO into black graphene at precise locations. The laser scribing technology makes it possible that the large-area of precise graphene patterns can be obtained in ~25 minutes. (b) An original image of wafer-scale in-plane transistor patterns and (c) the same image reproduced by laser scribed graphene. (d) An original image of Tsinghua University logo [copyright permission from Tsinghua University] and (e) the same image reproduced by laser scribed graphene. (f) A standard complex colored image of graphene and (g) the same image reproduced by reducing graphite oxide at various levels, which corresponds to a change in electrical properties. (h) An array of graphene transistors, an array of photodetectors, and a graphene loudspeaker device integrated in a flexible substrate by the direct laser scribing method. (i) The devices on PET substrate with flexible. (j) Wafer-scale fabrication flexible graphene-based devices.

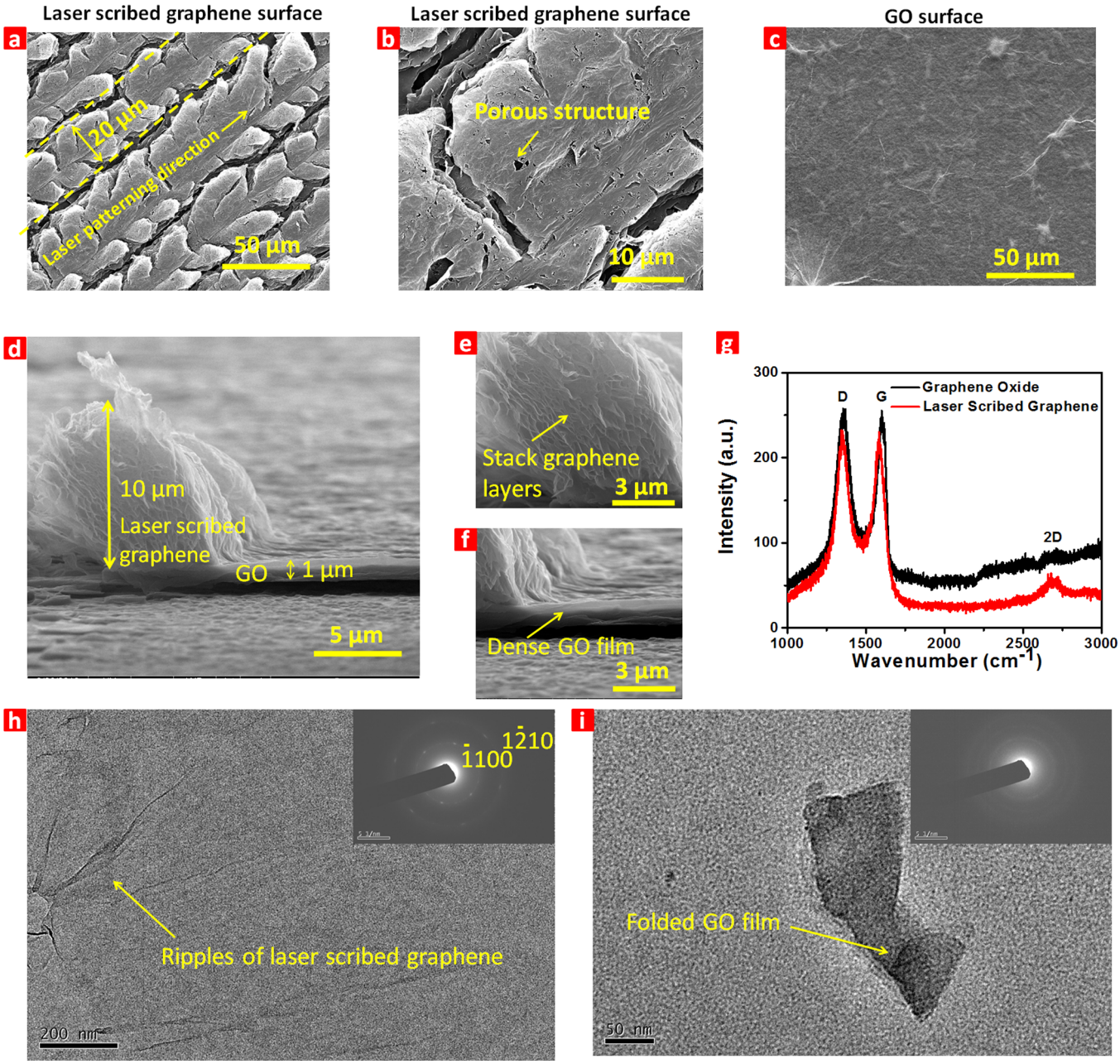

Figure 2 | The morphology and structure of the laser scribed graphene and GO film. (a) The SEM image of laser scribed graphene surface under low magnification. The laser scanning direction is shown. And the minimum patterning resolution of laser scribed graphene is 20 μm. (b) The SEM image of laser scribed graphene surface under high magnification. (c) The surface profile of GO film under SEM. (d) Cross-sectional view of GO and laser scribed graphene film. An increase in laser scribed graphene film thickness is clearly visible. (e) The zoom-in cross-sectional view of laser scribed graphene film under high magnification. An stack graphene layers could be clearly indentified. (f) The zoom-in cross-sectional view of GO film under high magnification. (g) The Raman spectrum of the GO (black line) and laser scribed graphene (red line). Compared with GO, the increase in 2D band of laser scribed graphene indicates that few-layers graphene generated after laser irradiation. (h) A TEM image of single-layer laser scribed graphene deposited on carbon TEM grids. Electron diffraction on the graphene film is shown as an inset. (i) A TEM image of few-layer GO film deposited on carbon TEM grids. Electron diffraction on the GO film is shown as an inset.

expanding by gasification of oxygen species. The surface profile of GO film before laser scribed is shown in Figure 2c, which indicates that the film is quite uniform with small roughness. As shown in Figure 2d, an increase in laser scribed graphene film thickness is clearly visible in the cross-sectional view of GO and laser scribed graphene film. The thickness of laser scribed graphene, which is 10 times of the GO film, indicates that a significantly volume expansion related to the gasification of oxygen species possibly could happen in thickness direction of the GO film during the laser irradiation. The loosely stacked graphene layers could be clearly identified in Figure 2e, the cross-sectional view of rGO film under high magnification. As can be seen from the cross-sectional view of GO film under high magnification (Figure 2f), the GO film is quite dense, which is quite different from the loosely stacked graphene layers. Differently, for conventional method to reduce the GO, the temperature applied on GO is increased slowly. The oxygen could release slowly from reduced graphene oxide to form dense film. Therefore, the thickness of the dense reduce graphene oxide will decrease smoothly due to the loss of oxygen functional group[9]. In this work, the laser could give a thermal pulse to GO to increase its

temperature in a short time, which is quite different from conventional method. The increase in thickness could be explained by the rapid generation and release oxygen gases during laser irradiation. When short-time laser treats on small area of GO, the temperature of GO could increase in a short time. As a result, gases rapidly pass through the film, which could effectively cause the reduced graphene oxide expanding in thickness direction. This process is similar to thermal shock. As shown in figure 2e, the distance between graphene layers are hundreds of nm, which is loose. There is enough path ways for gas passing away.

The Raman spectra of the GO (black line) and laser scribed graphene (red line) is shown in Figure 2g. GO exhibiting typical D, G, and amorphous 2D bands. It is noticed that there is no obvious D band change after the laser scribing. The GO is the carbon lattice with defect contain oxygen functional groups. The oxygen functional groups break the C-C bond to form obvious D band. After the laser scribing, the C-oxygen functional groups bond break and oxygen is released. Since there is 10 times thickness expand after laser scribing and laser scribed graphene is loose stack films, C-C recombination is difficult. Hense, there is no obvious change in D band. It is also noticed that the G band shift to smaller wavenumber, which is due to the reduction of oxygen functional group. The presence of the 2D band indicates the generation of few-layer graphene. Figure 2h is the TEM image of single-layer laser scribed graphene deposited on carbon TEM grids. The inset of electron diffraction on the graphene film reveals a hexagonal pattern, which indicates the crystallinity of the graphene. Figure 2i is the TEM image of few-layer GO film deposited on carbon TEM grids. The inset of electron diffraction on the GO film shows blurred rings. The XPS results of laser scribed graphene and GO are shown in Supplementary Information as Figure S1. Compared with graphene oxide, it is noticed that oxygen functional group is reduced while C-C sp^2 and π-π^* bonding are increased significantly in laser scribed graphene[17]. The laser scribed graphene micro-ribbon with a minimum patterning resolution of 20 μm is shown in Supplementary Information as Figure S2. The sheet resistance of the graphene micro-ribbon is about 165 Ω per square, which is indicated in the two-probe electrical measurement of the laser scribed graphene micro-ribbon (20 μm width) in Supplementary Information as Figure S3.

Tunable resistance of laser scribed graphene. Two-probe electrical testing are performed on the GO for the sake of demonstrating the electrical resistance tunable ability. And three laser scribed graphene samples which are scribed different times respectively. The electrical experimental results of the GO film and laser scribed graphene with one, two and three scribing times are shown in Figure 3. The I-V cure of GO film (Figure 3a) indicates its resistance is 580 MΩ, which means the film could be considered as an insulator. With reference

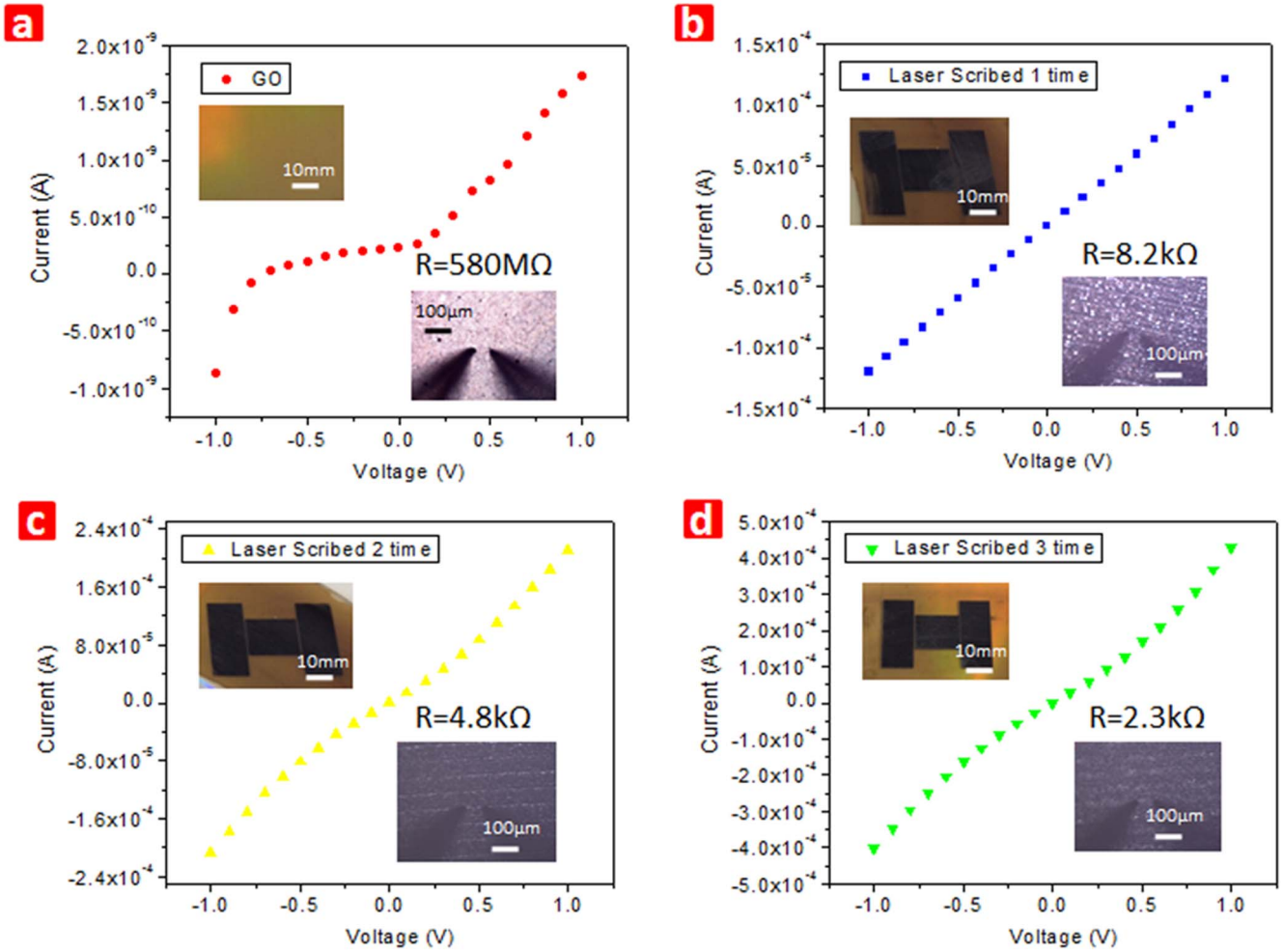

Figure 3 | The electrical experimental results of the GO film and laser scribed graphene. (a) The I-V cure of GO film. The resistance is 580 MΩ, which could be regarded as an insulator. (b) The I-V cure of graphene after 1 time laser scribing. The resistance reduces to 8.2 kΩ significantly. (c) The I-V cure of graphene after 2 times laser scribing. The resistance reduces to 4.8 kΩ. (d) The I-V cure of graphene after 3 times laser scribing. The resistance reduces to 2.3 kΩ. The upper inset photograph is the GO film and laser scribed graphene after patterning 1 time, 2 times and 3 times, respectively. Lower inset photograph showing two probes testing on the films.

to the I-V cure of laser scribed graphene after one-time patterning (Figure 3b), the resistance significantly reduces to 8.2 kΩ, which is almost five orders of magnitude decrease compared with GO. Similarly, the resistance of the laser scribed graphene after two-times patterning reduces to 4.8 kΩ, which is indicated by the I-V cure in Figure 3c. The resistance of laser scribed graphene after three-times patterning reduces to 2.3 kΩ, which is indicated by the I-V cure in Figure 3d.

Direct fabrication of in-plane all-graphene transistors. Previously, most of graphene-based transistors are either back-gate or top gate[18–20]. Since the back-gate controlling the whole devices, the back-gate transistors have problem of lacking the single transistor control ability. Top-gate graphene-based transistors could be fabricated with high-k dielectric deposition and metal gate patterning with complex process. Here, we demonstrated a one-step fabrication process of laser scribed in-plane graphene transistors. This kind of graphene-based in-plane transistor has the advantages of simple process and single transistor control ability. In this in-plane transistor, the laser scribed graphene functions as source, drain, channel and gate-metal and the GO functions as gate dielectric.

The schematic diagrams and experimental results for a laser scribed in-plane graphene transistor are sketched in Figure 4. The fabrication process for a laser scribed in-plane graphene transistor is depicted in the schematic diagram in Figure 4a. The transfer characteristic for the in-plane graphene transistor with 0.1 V applied bias voltage V_{ds} is indicated in Figure 4b. As seen in the graph, the I_{on}/I_{off} is up to 5.34, which is much higher than that of most CVD graphene transistors[13–15,21] and similar to performance of exfoliated graphene[22,23]. The transfer curve shows the holes transport with 9.87 $cm^2V^{-1}s^{-1}$ mobility (See detail calculations of the mobility in Supplementary Information). As the structure defects exist in laser scribed graphene, the low mobility could be reasonable and is similar to the reported results[24]. It should be noted that the Dirac point shifts larger than 40 V, which could be explained by the present of residual oxygens those dope the graphene into highly p-type. The frequency dependence of the specific capacitance of the capacitor in graphene/GO in-plane graphene configuration is shown in Figure S4. As can be seen, the capacitance at 1 kHz frequency is 6.34×10^{-4} Fm^{-2}. The I_{ds}–V_{ds} curve recorded for different values of V_{ig} is shown in Figure 4c. Positive gate voltage could lead to lower current and negative gate voltage makes the current higher, which is consistant with the transfer curve shown in fig. 4b.

Direct fabrication of graphene-based photodetector. Photoresponse in graphene has been extensively investigated[25–30] due to graphene's wide-band light absorption ability. F. Xia et al. made ultrafast graphene-based photodector by applying laser on graphene field effect transistor[31]. Nevertheless, the photo responsivity of the previous graphene photodetectors is too low (typically 0.004 A/W)[32]. Konstantatos et al. demonstrated 10^7 A/W photodector by using graphene and quantum dot hydrid system. Quantum-dot layer absorbs the light, creates electric charges and then transfers to the graphene. The graphene was used as charge transfer layer. Despite all that, how to enhance the pure graphene photo current is still a critical problem. In this work, stack graphene layer is used to enhance the light absorption. We directly fabricated photodetector using laser scribed graphene with photo responsivity as high as 0.32 A/W, which is almost two order of magnitude enhancement over the pure graphene result.

The schematic diagrams and experimental results for a laser scribed graphene photodetector is illustrated in Figure 5. Figure 5a

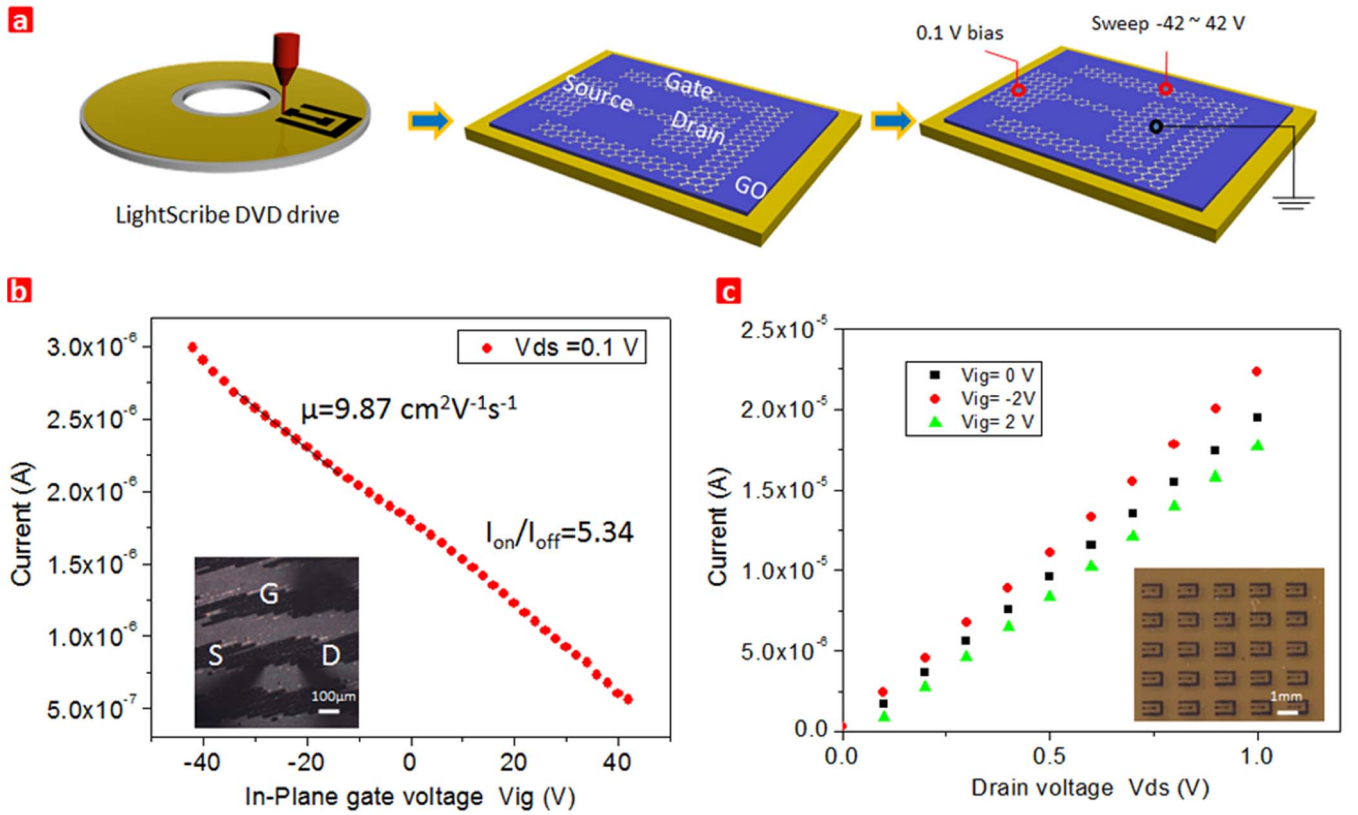

Figure 4 | Schematic diagrams and experimental results for a laser scribed graphene in-plane transistors. (a)Schematic diagram of the fabrication process and testing condition for a laser scribed in-plane graphene transistor. (b) Transfer characteristic for the in-plane graphene transistor with 0.1 V applied bias voltage V_{ds}. Inset showing the in-plane transistor with three-terminal probing. (c) I_{ds}–V_{ds} cure recorded for different values of in-plane gate voltage V_{ig}. The inset is a 5 × 5 array of the in-plane graphene transistor.

is a schematic diagram showing the fabrication process for a laser scribed graphene photodetector. The I-V curves under laser on and off is shown in Figure 5b, which demonstrated that the positive photocurrent generated when apply laser compared with laser off line. The inset shows the experimental setup for testing the photodetector. As can be seen in the current versus time under dark and laser cycling in Figure 5c, the photocurrent increases and becomes saturate in a short time when applying light. And the photocurrent decreases to the initial level when the laser is off. The photo current mapping by changing laser intensity shown in Figure 5d indicates that higher laser intensity could induce larger photocurrent. The line in the plot of the photo intensity versus the photocurrent (Figure 5e) indicates that the photocurrent increases linearly with the increasing of the laser intensity. The current response to turning on/off shows exponential rise/fall behaviors (See Supporting information Figure S5, S6). The turning on and off time are 1.45 s and 2.79 s respectively. The photovoltaic effect could be the main mechanism of photocurrent generation in our case (See Supporting information Figure S7, S8).

As the laser scribed graphene could be done in large-scale with precious dimensions, 1-dimensional and 2-dimensional array of photodetectors could be achieved by this method. The schematic structure of a 1-dimensional array of the photodetectors with a light source applied at one end of the array is illustrated in Figure 5f. The inset shows the real optical image of the 23 pixels array. The length and width of each device are 250 μm and 3000 μm, respectively. The center to center spacing of the neighboring devices is 500 μm. As the photo current versus the position of the detector from the light shown in Figure 5g, the photocurrent decreases with the increase of the distance from the light source. The inset shows the 1-dimensional pixilation plot, where each pixel is represented by a device in the array. The schematic structure of a 2-dimentional array of the photodetectors under a light source at center of the array is depicted in Figure 5h. The inset shows the real optical image of the 3×3 pixels array. The 2-dimensional pixilation plot of the 3×3 array is shown in Figure 5i. The asymmetric patterns are due to the dispersion of the light source. It is noticed that the signal in the center is the strongest and the signal is decreased with increasing of the distance from the center.

Direct fabrication of graphene-based loudspeakers. Previously, all the reported graphene loudspeakers need CVD graphene growth and transfer process[16,33–35], which is time consuming and of low efficiency. A scalable fabrication process for graphene loudspeakers by laser scribing technology is proposed here.

The schematic diagrams and experimental results for a laser scribed graphene loudspeaker is shown in Figure 6. The fabrication process and experimental setup for a laser scribed graphene loudspeaker is illustrated in the schematic diagram shown in Figure 6a. 5 V sine signal sweep from 1 to 50 kHz with 5 V bias is applied to graphene to generate the same frequency sound waves. As we can see in the sound spectrum of the graphene loudspeaker (Figure 6b), for 1 to 20 kHz region, the values of sound pressure level (SPL) increase linear with the frequency. And for 20 to 50 kHz region, the SPLs are quite flat. The inset shows the experimental setup for testing the loudspeaker. The overall trend in the sound spectrum mapping by sweeping the input power (Figure 6c) indicates that the SPLs increase with the input power. And the overall trend in the sound spectrum mapping by sweeping the measure distance (Figure 6d) indicates that the SPLs decrease with the measure distance. The line in the plot of the sound pressure versus the input power at 20 kHz sound frequency (Figure 6e) demonstrates that the output sound pressure increases linearly with the increasing of the input power. The line in the plot of the sound pressure versus the measure distance at 20 kHz sound frequency (Figure S9) demonstrates that there is an inverse relationship between the output sound pressure and measure distance. The thermoacoustic effect could be the main mechanism of sound generation in our case (See Supporting information Figure S10).

Discussion

The novelty of this work is the integrating of wafer-scale high-performance graphene-based in-plane transistors, photodetectors and loudspeakers with one-step fabrication. The achievements in our work are mainly four parts. Firstly, a laser scribing technology to fabricate wafer-scale grapheme was developed. This laser scribing technology has the advantages of forming graphene in designed shape at precise locations, low cost with large scale fabrication ability and simple process. Secondly, laser scribed graphene was used to realize all graphene-based large-scale in-plane transistors with high I_{on}/I_{off} ratio, this parameter is better than that of most CVD graphene[13–15] (I_{on}/I_{off} ratio $\sim$1.04 $\sim$ 1.4). Thirdly, the large-scale photodetectors and line pixels imaging with high photo responsivity were achieved with the laser scribed graphene. As far as we know, this is the first demonstration 1-dimentional and 2-dimentional array of graphene photodetectors for photo imaging. In addition, the responsivity of photodetectors is 2 orders magnitude, which is much better than that of the reported rGO[32]. Fourthly, the sound generation in a wide range was realize with laser scribed graphene, of which the sound generation spectrum (1–50 kHz) is 2.5 times wider than that of reported mono-layer graphene on PDMS (1–20 kHz)[16].

For graphene in-plane transistors, the higher on/off ratio is on account of the band gap opening of the laser scribed graphene. However, for CVD graphene, there is no band gap. Since GO has a bad gap larger than 0.5 eV and GO could be partly reduced by the laser, there is band gap for the laser scribed graphene, which could make higher I_{on}/I_{off} ratio than conventional CVD graphene. The defect in laser scribed graphene is obvious with strong D peak in Raman spectrum, result in the low mobility. The thermal annealing may enhance the mobility to a more reasonable value. The laser scribed graphene is highly p-doped. In order to make the Dirac-point shift to zero, the chemical n-type doper such as Al could be utilized. For graphene photodetectors, the enhancement of photo responsibility could be explained by the increasing the density of trap states due to the defects in laser scribed graphene. This could lead to an increase in carrier injection and transport, thereby producing a larger photo current. For graphene loudspeaker, the wide-band graphene sound generation is attributed to the thermoacoustic effect. Graphene could emit sound without mechanical vibration, which is fundamental different from conventional acoustic devices.

There is a lot of further work could be achieved. Current resolution of the DVD laser scribing is 20 μm. Smaller resolution is necessary to grow graphene nanoribbon with higher band gap. Smaller laser spot or even e-beam systems could realize nanoscale resolution. Connection between the graphene multi-functional devices could be made to realize a graphene system. The compatible of laser scribing technology with other conventional CMOS fabrication process needs to be intensively investigated to make more complex graphene-Si hybrid systems.

Conclusion

From the discussion above, the wafer-scale direct fabrication of graphene-based transistors, photodetectors and loudspeakers are achieved with a common LightScribe DVD burner. By controlling the pattering times, the resistance of the graphene could be tuned. Laser scribed in-plane graphene transistors have been demonstrated to have a large on/off ratio up to 5.34. Photo responsivity and specific detectivity as high as 0.32 A/W and 4.996×10^{10} $cmHz^{1/2}W^{-1}$ have been observed in the laser scribed graphene photodetectors. Sound generation of laser scribed graphene is also well demonstrated ranging from 1 to 50 kHz sound frequency. This work indicates that

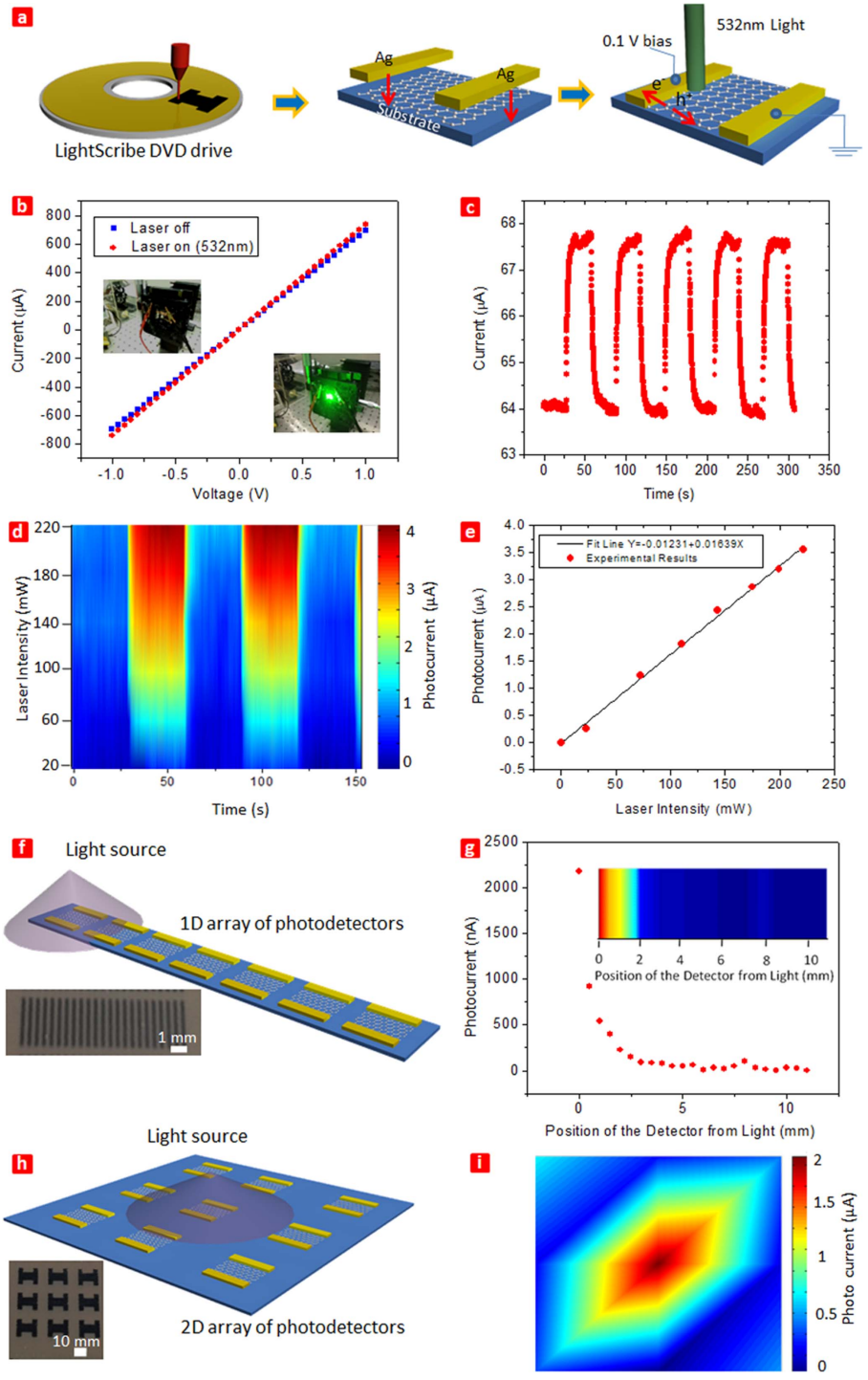

Figure 5 | Schematic diagrams and experimental results for laser scribed graphene photodetectors. (a) Schematic diagram of the fabrication process for a laser scribed graphene photodetector. (b) The I-V cures under laser on and off. Compared with dark line, it indicates that the positive photocurrent generated when apply light. The inset showing the experimental setup for testing the photo detector. The length and the width of the photodetector is 5 mm and 10 mm, respectively. (c) The time versus current under dark and light cycling. Both the dark and light last 30 s for each cycle. When applying light, it is noticed that the photocurrent increase and become saturate in a short time. After dark, the photocurrent decrease and back to original state. (d) The photocurrent mapping by changing photo intensity. Both the dark and light last 30 s for each cycle. It is indicated that larger photo intensity could induce higher photo current. (e) The plot of the photo intensity versus the photo current. The line shows that the photo current increases linearly with the increasing of the photo intensity. (f) Schematic structure of a line array of the photodetectors under a light source put at one end of the array. Inset showing the real photo the 23 pixels array. The length and width of the device are 250 μm and 3000 μm, respectively. The center to center spacing with each devices is 500 μm. (g) Photo current versus the position of the detector from the light. The inset showing the 1-dimensional pixilation plot, where each pixel is represented by a device in the array. The photocurrent is decreased with the increasing the distance from the light source. (h) Schematic structure of a 2-dimentional array of the photodetectors under a light source put at center of the array. Inset showing the real photo the 3 × 3 pixels array. (i) 2-dimensional pixilation plot of the 3 × 3 array.

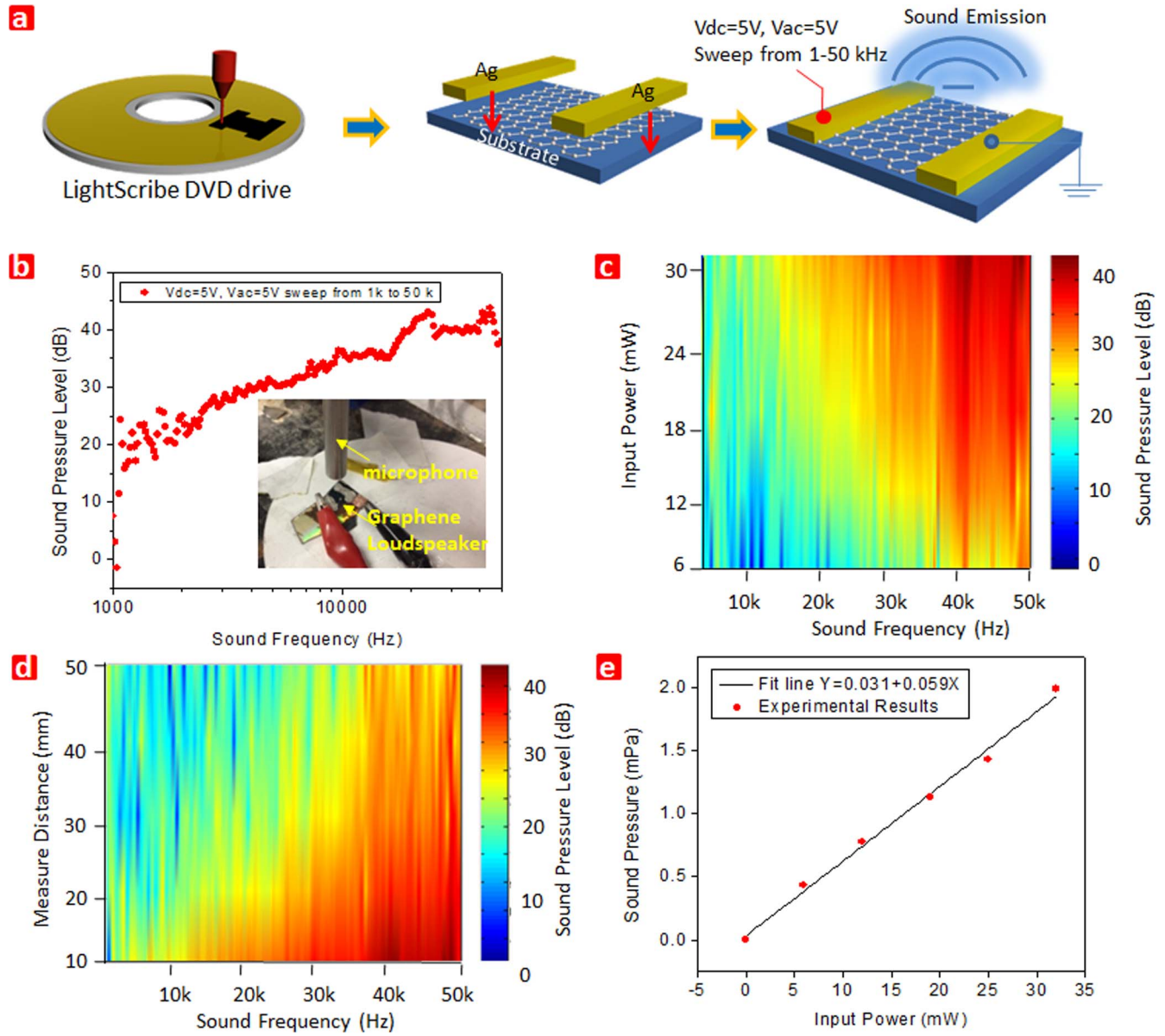

Figure 6 | Schematic diagrams and experimental results for a laser scribed graphene loudspeaker. (a) Schematic diagram showing the fabrication process for a laser scribed graphene loudspeaker. 5 V sine signal sweep from 1 to 50 kHz with 5 V bias is applied to graphene to generate the sound waves. (b) The sound frequency spectrum of the graphene loudspeaker. For 1 to 20 kHz region, the values of sound pressure level (SPL) increase linear with the frequency. For 20 to 50 kHz region, the SPLs are quite flat. Inset showing the experimental setup for testing the loudspeaker. (c) The sound spectrum mapping by sweeping the input power. The overall trend is that the SPLs increase with the input power. (d) The sound spectrum mapping by sweeping the measure distance. The overall trend is that the SPLs decrease with the measure distance. (e) The plot of the sound pressure versus the input power at 20 kHz sound frequency. The line in the plot indicates that the output sound pressure increases linearly with the increasing of the input power.

laser scribing technology could be a powerful and efficient method to integrate high-performance graphene-based devices.

Methods

Material preparation. GO dispersion in water with 2 mg/ml concentration was purchased from XFNANO Materials Tech CO., Ltd (Nanjing, China). GO solutions were synthesized from the graphite powders using a common Hummers method. About 10 mL GO solutions were drop-casted on the surface of the laser-scribed DVD disc. Then leave the GO solutions overnight to dry on the DVD disc. After that, the GO coated DVD disc could be patterned by the light-scribed DVD Drive (HP inc. 557S). With the Nero Start Smart software, the designed structure or photograph could be directly converted onto the GO film by laser reducing the GO into graphene.

To fabricate the flexible devices, firstly cover a PET on DVD disc, then drop-casted GO solution and finally laser scribed graphene-based devices and peel it off from the DVD disc.

Characterizations. The surface morphology is observed by Quanta FEG 450 SEM (FEI Inc.). The Raman spectroscopy is obtained using a laser with wavelength of 514.5 nm (HORIBA Inc.).The XPS is captured by EscaLab 250XI (Thermo Fisher Scientific Inc.).

Testing for in-plane transistors. The electrical testing was done by a standard probe station (Agilent inc. B1500).

Testing for photo-detectors. The laser was irradiated on the boundary of the laser-scribed graphene and Ag electrode. The wavelength of the laser was 532 nm. Photocurrents were measured using a sourcemeter (Keithley 2400).

Testing for loudspeakers. The acoustic platform for testing laser scribed graphene loudspeakers contained a standard microphone and a dynamic signal analyzer. The 1/4 inch standard microphone (Earthworks M50), which had a very flat frequency response reaching up to 50 kHz and a 31 mV/Pa high sensitivity, was used to measure the sound pressure level of the loudspeakers. The signal analyzer (Agilent 35670A)

was used to generate sine signals to drive loudspeakers, make fast Fourier transform analysis and record the value of sound pressure level. Our test results were measured in a soundproof box. The box size is $1 \times 0.5 \times 0.5$ m^3. In order to avoid the effects of reflections, the box was filled with sound-absorbing sponges.

1. Geim, A. K. & Novoselov, K. S. The rise of graphene. *Nat. Mater.* **6**, 183–191 (2007).
2. Bolotin, K. I. *et al.* Ultrahigh electron mobility in suspended graphene. *Solid State Communications* **146**, 351–355 (2008).
3. Lee, C., Wei, X., Kysar, J. W. & Hone, J. Measurement of the elastic properties and intrinsic strength of monolayer graphene. *Science* **321**, 385–388 (2008).
4. Balandin, A. A. *et al.* Superior thermal conductivity of single-layer graphene. *Nano Lett.* **8**, 902–907 (2008).
5. Bae, S. *et al.* Roll-to-roll production of 30-inch graphene films for transparent electrodes. *Nat. Nanotechnol.* **5**, 574–578 (2010).
6. Meric, I. *et al.* Current saturation in zero-bandgap, top-gated graphene field-effect transistors. *Nat. Nanotechnol.* **3**, 654–659 (2008).
7. Wu, X. *et al.* Epitaxial-graphene/graphene-oxide junction: an essential step towards epitaxial graphene electronics. *Physical review letters* **101**, 026801 (2008).
8. Eda, G., Fanchini, G. & Chhowalla, M. Large-area ultrathin films of reduced graphene oxide as a transparent and flexible electronic material. *Nat. Nanotechnol.* **3**, 270–274 (2008).
9. Wei, Z. *et al.* Nanoscale tunable reduction of graphene oxide for graphene electronics. *Science* **328**, 1373–1376 (2010).
10. Gao, W. *et al.* Direct laser writing of micro-supercapacitors on hydrated graphite oxide films. *Nat. Nanotechnol.* **6**, 496–500 (2011).
11. El-Kady, M. F. & Kaner, R. B. Scalable fabrication of high-power graphene micro-supercapacitors for flexible and on-chip energy storage. *Nature communications* **4**, 1475 (2013).
12. Tian, H. *et al.* Scalable fabrication of high-performance and flexible graphene strain sensors. *Nanoscale*, DOI: 10.1039/c3nr04521h (2014).
13. Reina, A. *et al.* Large area, few-layer graphene films on arbitrary substrates by chemical vapor deposition. *Nano Lett.* **9**, 30–35 (2008).
14. Yan, Z. *et al.* Growth of bilayer graphene on insulating substrates. *ACS nano* **5**, 8187–8192 (2011).
15. Kwak, J. *et al.* Near room-temperature synthesis of transfer-free graphene films. *Nature communications* **3**, 645 (2012).
16. Suk, J. W., Kirk, K., Hao, Y., Hall, N. A. & Ruoff, R. S. Thermoacoustic sound generation from monolayer graphene for transparent and flexible sound sources. *Advanced Materials* **24**, 6342–6347 (2012).
17. Strong, V. *et al.* Patterning and electronic tuning of laser scribed graphene for flexible all-carbon devices. *ACS nano* **6**, 1395–1403 (2012).
18. Lin, Y.-M. *et al.* 100-GHz transistors from wafer-scale epitaxial graphene. *Science* **327**, 662–662 (2010).
19. Das, A. *et al.* Monitoring dopants by Raman scattering in an electrochemically top-gated graphene transistor. *Nat. Nanotechnol.* **3**, 210–215 (2008).
20. Schwierz, F. Graphene transistors. *Nat. Nanotechnol.* **5**, 487–496 (2010).
21. Wang, D. *et al.* Scalable and Direct Growth of Graphene Micro Ribbons on Dielectric Substrates. *Scientific Reports* **3**, 1348 (2013).
22. Novoselov, K. *et al.* Electric field effect in atomically thin carbon films. *Science* **306**, 666–669 (2004).
23. Novoselov, K. *et al.* Two-dimensional gas of massless Dirac fermions in graphene. *Nature* **438**, 197–200 (2005).
24. Zhang, K. *et al.* Direct writing of electronic devices on graphene oxide by catalytic scanning probe lithography. *Nature communications* **3**, 1194 (2012).
25. Mueller, T., Xia, F. & Avouris, P. Graphene photodetectors for high-speed optical communications. *Nature Photonics* **4**, 297–301 (2010).
26. Furchi, M. *et al.* Microcavity-integrated graphene photodetector. *Nano letters* **12**, 2773–2777 (2012).
27. Urich, A., Unterrainer, K. & Mueller, T. Intrinsic response time of graphene photodetectors. *Nano letters* **11**, 2804–2808 (2011).
28. Bonaccorso, F., Sun, Z., Hasan, T. & Ferrari, A. Graphene photonics and optoelectronics. *Nature Photonics* **4**, 611–622 (2010).
29. Liu, Y. *et al.* Plasmon resonance enhanced multicolour photodetection by graphene. *Nature communications* **2**, 579 (2011).
30. Gabor, N. M. *et al.* Hot carrier–assisted intrinsic photoresponse in graphene. *Science* **334**, 648–652 (2011).
31. Xia, F., Mueller, T., Lin, Y.-m., Valdes-Garcia, A. & Avouris, P. Ultrafast graphene photodetector. *Nat. Nanotechnol.* **4**, 839–843 (2009).
32. Chitara, B., Panchakarla, L., Krupanidhi, S. & Rao, C. Infrared photodetectors based on reduced graphene oxide and graphene nanoribbons. *Advanced Materials* **23**, 5419–5424 (2011).
33. Tian, H. *et al.* Graphene-on-paper sound source devices. *ACS nano* **5**, 4878–4885 (2011).
34. Tian, H. *et al.* Single-layer graphene sound-emitting devices: experiments and modeling. *Nanoscale* **4**, 2272–2277 (2012).
35. Tian, H. *et al.* Static behavior of a graphene-based sound-emitting device. *Nanoscale* **4**, 3345–3349 (2012).

Acknowledgments

This work was supported by the National Natural Science Foundation of China (61025021, 60936002, 51072089, and 61020106006), the National Key Project of Science and Technology (2011ZX02403-002) the Special Fund for Agro-scientific Research in the Public Interest (201303107). He Tian is additionally supported by the Ministry of Education Scholarship of China. Thanks for the valuable discussions with Prof. Z. Bao from Stanford University.

Author contributions

H.T. made and tested the samples, performed simulations, and drafted the manuscript. T.-L.R. and Y.Z. oversaw all research phases, optimized the devices performance and revised the manuscript. D.X., Y.Y., Y.-L.C. and W.-T.M. analyzed the test results and revised the manuscript. All authors discussed and commented on the manuscript.

Additional information

Supplementary information accompanies this paper at http://www.nature.com/scientificreports

Competing financial interests: The authors declare no competing financial interests.

How to cite this article: Tian, H. *et al.* Wafer-Scale Integration of Graphene-based Electronic, Optoelectronic and Electroacoustic Devices. *Sci. Rep.* **4**, 3598; DOI:10.1038/srep03598 (2014).